Cytotherapy 000 (2024) 1–12

Contents lists available at ScienceDirect

CYTOTHERAPY

journal homepage: www.isct-cytotherapy.org

Full-length article

Proteomics of serum-derived extracellular vesicles are associated with the severity and different clinical profiles of patients with COVID-19: An exploratory secondary analysis

Adriana F. Paes Leme[1], Sami Yokoo[1], Ana Gabriela C. Normando[1], João Vitor S. Ormonde[1], Romenia Ramos Domingues[1], Fernanda F. Cruz[2,3,4], Pedro L. Silva[2,3,4], Bruno S.F. Souza[5,6,7], Claudia C. dos Santos[8,9], Hugo Castro-Faria-Neto[10], Camila Marinelli Martins[11], Miquéias Lopes-Pacheco[2,12], Patricia R.M. Rocco[2,3,4,*]

[1] *Laboratório Nacional de Biociências - LNBio, Centro Nacional de Pesquisa em Energia e Materiais - CNPEM, Campinas, São Paulo, Brazil*
[2] *Laboratory of Pulmonary Investigation, Carlos Chagas Filho Institute of Biophysics, Federal University of Rio de Janeiro, Rio de Janeiro, Brazil*
[3] *National Institute of Science and Technology for Regenerative Medicine, Rio de Janeiro, Brazil*
[4] *Rio de Janeiro Innovation Network in Nanosystems for Health-NanoSaúde, Research Support Foundation of the State of Rio de Janeiro, Rio de Janeiro, Brazil*
[5] *Goncalo Moniz Institute, Oswaldo Cruz Foundation (FIOCRUZ), Salvador, Bahia, Brazil*
[6] *D'Or Institute for Research and Education (IDOR), Salvador, Bahia, Brazil*
[7] *Center for Biotechnology and Cell Therapy, São Rafael Hospital, Salvador, Bahia, Brazil*
[8] *The Keenan Research Centre for Biomedical Science of St. Michael's Hospital, Toronto, Ontario, Canada*
[9] *Institute of Medical Sciences and Interdepartmental Division of Critical Care, Faculty of Medicine, University of Toronto, Toronto, Ontario, Canada*
[10] *Immunopharmacology Laboratory, Oswaldo Cruz Institute (FIOCRUZ), Rio de Janeiro, Brazil*
[11] *AAC&T Research Consulting LTDA, Curitiba, Brazil*
[12] *Biosystems & Integrative Sciences Institute, Faculty of Sciences, University of Lisbon, Lisbon, Portugal*

ARTICLE INFO

Article History:
Received 12 November 2023
Accepted 1 February 2024
Available online xxx

Key Words:
biomarkers
extracellular vesicles
mass spectrometry
platelet degranulation
proteome
SARS-CoV-2

ABSTRACT

Background aims: Coronavirus disease 2019 (COVID-19) is characterized by a broad spectrum of clinical manifestations with the potential to progress to multiple organ dysfunction in severe cases. Extracellular vesicles (EVs) carry a range of biological cargoes, which may be used as biomarkers of disease state.
Methods: An exploratory secondary analysis of the SARITA-2 and SARITA-1 datasets (randomized clinical trials on patients with mild and moderate/severe COVID-19) was performed. Serum-derived EVs were used for proteomic analysis to identify enriched biological processes and key proteins, thus providing insights into differences in disease severity. Serum-derived EVs were separated from patients with COVID-19 by size exclusion chromatography and nanoparticle tracking analysis was used to determine particle concentration and diameter. Liquid chromatography coupled with tandem mass spectrometry (LC-MS/MS) was performed to identify and quantify protein signatures. Bioinformatics and multivariate statistical analysis were applied to distinguish candidate proteins associated with disease severity (mild versus moderate/severe COVID-19).
Results: No differences were observed in terms of the concentration and diameter of enriched EVs between mild (n = 14) and moderate/severe (n = 30) COVID-19. A total of 414 proteins were found to be present in EVs, of which 360 were shared while 48 were uniquely present in severe/moderate compared to mild COVID-19. The main biological signatures in moderate/severe COVID-19 were associated with platelet degranulation, exocytosis, complement activation, immune effector activation, and humoral immune response. Von Willebrand factor, serum amyloid A-2 protein, histone H4 and H2A type 2-C, and fibrinogen β-chain were the most differentially expressed proteins between severity groups.
Conclusion: Exploratory proteomic analysis of serum-derived EVs from patients with COVID-19 detected key proteins related to immune response and activation of coagulation and complement pathways, which are associated with disease severity. Our data suggest that EV proteins may be relevant biomarkers of disease state and prognosis.

Introduction

Severe acute respiratory syndrome-coronavirus-2 (SARS-CoV-2) infection can cause a broad spectrum of clinical manifestations,

* Correspondence: Patricia R.M. Rocco, Laboratory of Pulmonary Investigation, Carlos Chagas Filho Institute of Biophysics, Federal University of Rio de Janeiro, Avenida Carlos Chagas Filho, 373, Bloco G-014, Ilha do Fundão, 21941-902, Rio de Janeiro, RJ, Brazil.
E-mail address: prmrocco@biof.ufrj.br (P.R.M. Rocco).

https://doi.org/10.1016/j.jcyt.2024.02.001
1465-3249/

which were predominant during the coronavirus disease 2019 (COVID-19) pandemic [1]. This virus has infected over 700 million people worldwide [2], and although most individuals are asymptomatic or present mild symptoms, in more severe cases, patients can develop pneumonia, acute respiratory distress syndrome, and coagulopathies [3–5]. More than 40% of patients with severe COVID-19 can exhibit thrombo-inflammatory complications with a high incidence of deep vein thrombosis and multiple organ dysfunction [3–6]. As a consequence, severe COVID-19 usually progresses to death (>6.9 million lives to date) [2] or disability with post-COVID sequelae syndrome in survivors [7,8].

An increasing number of studies have provided information about the different clinical manifestations and progression of COVID-19 [1,3,4], and extensive efforts have been made to unravel the mechanisms underlying these different phenotypes of the disease and the multiple organ involvement in more severe cases [5,9,10]. Some key pathologic mechanisms include the dysregulation of immune responses against SARS-CoV-2 infection, epithelial and endothelial cell injury, thrombo-inflammation, and significant tissue remodeling [5,6]. However, the underlying molecular mechanisms involved in the worsening of COVID-19 are still not completely understood [11,12]. Therefore, a deeper elucidation of pathways and potential targets involved in these mechanisms is still needed to assist in the prediction of disease severity, prognosis, and outcomes [13,14].

Extracellular vesicles (EVs) have emerged in recent years, not only as potential therapies [15–17] but also as relevant sources of biomarkers for different diseases [18]. EVs are cell-derived particles that include a lipid bilayer and their internal contents can reflect the physiologic or pathologic state of parental cells [19]. These structures are released by different cell types and are broadly transported through the bloodstream, acting with both paracrine and endocrine signals as newly recognized forms of intercellular communication [20]. Several proteomic studies have identified and quantified the protein cargo in EVs, thus unraveling the signaling pathways that are modulated in different pathologic conditions, including asthma [21], cancer [22], chronic obstructive pulmonary disease [23], and sepsis [24]. Mass spectrometry-based proteomic analysis also revealed marked differences in circulating EVs from patients with COVID-19 and healthy controls, enabling discrimination between these cohorts [25]. In EVs from patients with COVID-19, several biomarkers involved in inflammation, immune responses, and activation of complement and coagulation pathways were identified [25–27], highlighting the utility of EVs for better understanding the mechanisms of the disease and identifying biological processes and potential therapeutic targets. However, there is still a need to establish a set of key biomarkers using proteomics to better differentiate the severity of COVID-19 in patients and to correlate these proteins with patients; demographic and clinical profiles, such as age, sex, time from symptom onset, body mass index (BMI), and viral load.

In this study, we conducted an exploratory secondary analysis of the SARITA-1 (moderate/severe) [28] and SARITA-2 (mild) [29] datasets to better understand the relevant proteins in serum-derived EVs from patients with mild versus moderate/severe COVID-19 at the time of hospital admission and whether these proteins were correlated with the patient's clinical profile.

Materials and Methods

Study design and ethics

We conducted an exploratory secondary analysis of data from the SARITA-1 [28] and SARITA-2 [29] randomized clinical trials (RCTs) comparing nitazoxanide and placebo (control arm) in patients with moderate/severe and mild COVID-19, respectively. These trials were registered in ClinicalTrials.gov (NCT04561219 and NCT04552483, respectively), conducted following the Declaration of Helsinki and previously approved by the Brazilian National Commission for Research Ethics (CAAE: 32258920.0.1001.5257 and 30662420.0.1001.0008). SARITA-1 and SARITA-2 included adult (aged ≥18 years) patients with diagnoses of SARS-CoV2 confirmed by real-time reverse transcriptase polymerase chain reaction (RT-PCR). SARITA-1 (moderate/severe COVID-19) included hospitalized patients who required supplemental oxygen (peripheral oxygen saturation [SpO_2] <93%) and chest computed tomography (CT) suggestive of viral pneumonia. The SARITA-2 study (mild COVID-19) enrolled patients who had clinical symptoms of COVID-19 (dry cough, fever, and/or fatigue) for no more than 3 days.

Circulating EV proteome profile was assessed in 45 patients included in this study; 15 had mild and 30 had moderate/severe COVID-19. All these nontreated patients (control arm) from each study were pre-selected on the day of admission. The sample size of 45 was a result of a selection process to fulfill criteria from the original population of the two studies with 250 patients each (nontreated). In the SARITA-1 study, all patients admitted to the ICU in the first 48 h (n = 15) were included [28]. In order to have the same number of patients in each group, patients with moderate COVID-19 (n = 15) were selected using a random generator, considering the highest viral load as well as the levels of D-dimer and C-reactive protein (CRP) at the time of admission. All these patients recovered with no need for ICU admission. In the SARITA-2 study [28], 15 patients were also randomly selected, but because one patient's sample was lost during preparation procedures, the final number was 14. Thus, 44 patients were studied.

The following clinical and laboratory variables were available for analysis: age, sex, BMI, time from symptom onset, and CRP level.

Blood sample collection, serum separation, and EV purification by size exclusion chromatography

Whole blood (20 mL) was drawn from a peripheral vein into two specimen tubes containing protease inhibitors (1 mM EDTA and 1 mM phenylmethylsulfonyl fluoride). The tubes were first centrifuged at 2000 × g for 10 min in a refrigerated centrifuge to separate the serum. Thereafter, the serum samples were centrifuged at 10 000 × *g* for 10 min to remove cell debris. Serum-derived EVs were collected using a qEVoriginal/70-nm size exclusion chromatography (SEC) column (Izon Science, Christchurch, New Zealand) as previously described for similar clinical samples [30–33] and according to the manufacturer's protocol. Briefly, the qEV column was equilibrated with a 15-mL flow of phosphate-buffered saline (PBS) to flow through the column before sample loading. Five hundred microliters of serum was loaded onto the qEV column and allowed to flow into the resin. The serum layer was overlaid with 3 mL of PBS and the initial 2.5 mL of flow through containing the void volume was discarded, which corresponded to fractions 1–5 of 500 μL each. Individual fractions of 500 μL containing serum-derived EVs were then sequentially collected (fractions 6–10), as the column was gradually loaded with 7 mL of PBS. The column was then washed with a continuous flow of 45 mL of PBS in preparation for the next sample. Following the manufacturer's instructions, fractions 8 and 9 were selected for downstream applications based on their high EV number/serum protein ratio (Figure 1).

Nanoparticle tracking analysis

Enriched EVs from fractions 8 and 9 were characterized by nanoparticle tracking analysis (NTA) on a NanoSight NS3000 instrument (NanoSight, Malvern Panalytical, Amesbury, UK) equipped with a sample chamber with a 532-nm green laser. Aliquots of the enriched EVs were diluted 1000 times and measured at 18°C in ultrapure water to capture five videos for 60 s with camera gain adjustments appropriate for the best focus on the EVs [34]. NTA 3.4 build 3.4.4

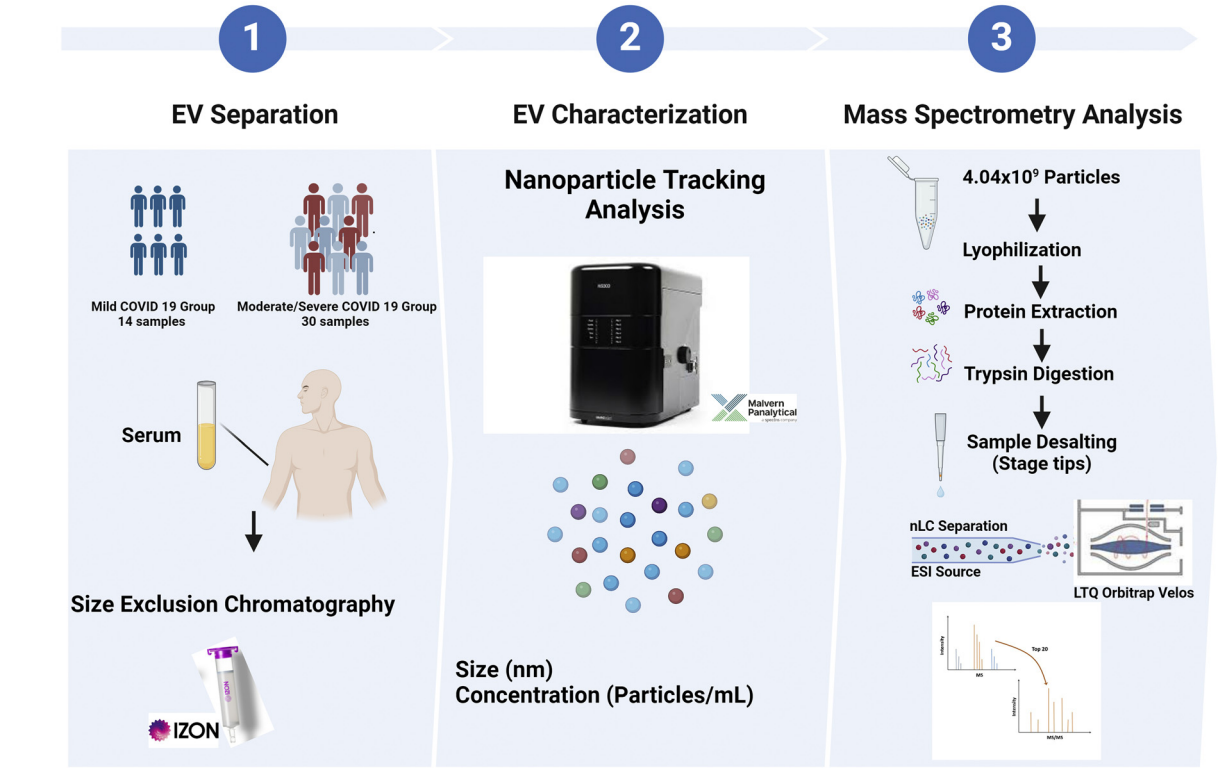

FIGURE 1. Experimental design for characterization of extracellular vesicles (EVs) separated and enriched from serum of patients with moderate/severe and mild COVID-19. Serum-derived EVs were separated using size exclusion chromatography, characterized by nanoparticle tracking analysis, analyzed using liquid chromatography/tandem mass spectrometry, and results associated with the clinical characteristics.

software was used for data acquisition and analysis. The size and concentration of the nanoparticles were determined based on the Brownian motion of the individual particles and light scattering measurements as previously reported [35].

Cryogenic electron microscopy (Cryo-EM)

Serum EV preparations from a pool of five patients from each group (severe, moderate, and mild COVID-19; 2.4×10^{10} particles/mL, 1.16×10^{10} particles/mL, and 1.08×10^{10} particles/mL, respectively) were suspended in PBS and 3 μL was used for image acquisition and sample analysis. Copper grids for electron microscopy were used with Lacey-type carbon film (300 mesh, #01895-F; Ted Pella, Reading, CA, USA). The grids were treated with a load of 25 mA for 50 s in EasiGlow (I) equipment (Ted Pella). The samples were plunge-frozen on a Vitrobot Mark IV (Thermo Fisher Scientific, Waltham, MA, USA). The samples were applied to each grid and the excess draining step was applied (blot time 3 and blot force 4); the grids were frozen immediately in liquid ethane and kept in liquid nitrogen until insertion into the microscope. All data were collected at an electron microscopy facility on a 200-kV Talos Arctica G2 (Thermo Fisher) equipped with an automatic system for storing and changing grids at cryogenic temperatures and a 4k × 4k CMOS camera (Thermo Fisher) for digital image acquisition.

Proteomic analysis of serum-derived EVs

After quantifying the EVs by NTA, 4.04×10^{9} particles were subjected to total lyophilization with a FreeZone 4.5 Liter Freeze Dry System (Labconco, Kansas City, MO, USA). Samples were treated with 8 M urea for protein extraction and digestion, followed by protein reduction with 5 mM dithiothreitol and alkylation with 14 mM iodoacetamide in the dark for 30 min. The reaction was quenched by adding 5 mM dithiothreitol and incubated in the dark for 15 min. Protein extracts were diluted to a final concentration of 1.6 M urea with 50 mM ammonium bicarbonate and 1 mM of calcium chloride. Thereafter, digestion with trypsin (Promega, Madison, WI, USA) was carried out in two steps; 500 ng of the enzyme was added for 16 h, followed by the addition of 500 ng for 5 h at 37°C. The reaction was quenched with 0.4% formic acid, and peptides were desalted using the StageTips method in C18 Empore disks (3M, St Paul, MN, USA) [36], dried in a vacuum concentrator, and reconstituted in 10 μL of 0.1% formic acid. Peptide quantification was obtained using a peptide digest standard provided by a Pierce Quantitative Colorimetric Peptide Assay (Thermo Fisher) to generate linear standard curves for calibration and peptide quantification. All measurements were performed at 280 nm using a NanoDrop 2000 spectrophotometer (Thermo Fisher).

Data acquisition by LC-MS/MS

An aliquot containing 1.5 μg of peptides for each sample was analyzed using an LTQ Orbitrap Velos mass spectrometer (Thermo Fisher) connected to an EASY-nLC II system (Proxeon Biosystem, West Palm Beach, FL, USA) through a Proxeon nanoelectrospray ion source. Peptides were separated with a 2%–90% acetonitrile gradient in 0.1% formic acid using an analytical PicoFrit Column (20 cm×75 μm inner diameter, 5 μm particle size; New Objective, Littleton, MA, USA) at a flow rate of 300 nL/min over 170 min. The nanoelectrospray voltage was set to 2.2 kV and the source temperature was 275°C. Full scan mass spectra (m/z 300–1600) were acquired in the Orbitrap analyzer after accumulation to a target value of 1×10^{6}. The resolution in the Orbitrap was set to r = 60 000 and the 20 most intense peptide ions with charge states ≥2 were sequentially isolated to a target

value of 5000 and fragmented in the linear ion trap using low-energy collision-induced dissociation (normalized collision energy of 35%). The signal threshold for triggering an MS/MS event was set to 1000 counts. Dynamic exclusion was enabled with an exclusion size list of 500, an exclusion duration of 60 s, and a repeat count of 1. An activation of q = 0.25 and an activation time of 10 ms were used.

Raw LC-MS/MS data analysis

Raw data were processed using MaxQuant v.2.0.1 software against the UniProt Human Protein Database (release January 2022; 100 730 sequences; 40 967 805 residues). A tolerance of 10 ppm for precursor mass and 1 Da for fragment ions was set for protein identification. Carbamidomethylation was set as a fixed modification and N-terminal acetylation and oxidation of methionine as variable modifications, a maximum of one trypsin missed cleavage, and matching between runs was set and applied with a 2-min window. Using Perseus v.2.0 software, the list of peptides identified was filtered by "only identified by site" entries and reverse sequences. Protein abundance was calculated based on the normalized spectrum intensity, label-free quantification (LFQ) intensity, transformed to log 2.

Bioinformatic data analysis

The overlay between molecules for each condition was visualized in a Venn diagram generated at http://www.interactivenn.net/. The hierarchical cluster heatmap was built in the R environment (v. 2022.12.0 build 353 and R 4.2.2) using Spearman distance with Ward linkage. Enrichment for Gene Ontology biological processes for protein cluster groups was determined in Enrichr (https://maayanlab.cloud/Enrichr/) using two-sided Fisher's exact test followed by Benjamini-Hochberg correction for multiple comparisons (adjusted p value < 0.05).

Data availability

The mass spectrometry proteomic data generated in this study are available at ProteomeXchange via the PRIDE partner repository [37] and Panorama repository. Data-dependent acquisition proteomics is available at ProteomeXchange with the dataset identifier, PXD041947.

Multivariate analysis

Initially, a descriptive and exploratory analysis was performed to compare the abundance differences in proteins between mild and moderate/severe COVID-19 along with clinical and sociodemographic variables using Fischer's exact test (categorical variables), Student's *t*-test (parametric), and Mann-Whitney's U test (nonparametric). Results were used to identify candidate proteins able to discriminate between groups of interest.

Multivariate analysis was then used to determine the association between the proteome and clinical severity phenotypes. A general linear model (GLM) with LASSO and elastic net regularization was used because it fits better for scatter and matrix data. The multivariate analysis was then performed to select the most relevant proteins. The CARET package (short for Classification And REgression Training) [38] was used for the computation because it has tuning techniques that identify the best combination for model parameters. A logistic regression model with a LASSO was implemented to verify the predictive potential of the proteins, and a K-fold cross-validation was performed to determine the lambda producing the best shrinkage of variables (i.e., the best way to determine only the most evident proteins). Thereafter, the mean squared error was estimated as a function of lambda, to identify a window close to zero, where the error is as small as possible. This window was considered in the next step.

The protein selection was carried out by calculating the beta coefficients of the regression model for each protein as a function of lambda, which generated a curve for their selection. Proteins with a coefficient different from zero were considered differentially present in EVs from mild versus moderate/severe COVID-19. At the end of this analysis, a random selection of patients was used to validate the accuracy and quality of the model. Cross-validation was used with k = 5 in relation to the accuracy and confusion matrix. The cross-validation technique was used to evaluate the model with k = 5 in relation to the accuracy and confusion matrix. Graphs of the received operating characteristic curve were produced, and sensitivity, specificity, and accuracy were calculated.

Correlations between selected proteins that differentiate mild versus moderate/severe COVID-19 and clinical characteristics were then performed. The differential percentage between mild versus moderate/severe COVID-19 was calculated (mild − [moderate/severe]/mild × 100) for each protein according to age groups (18–40 years, 41–59 years, and ≥60 years), time from symptom onset (0–5 days, 6–10 days, and ≥11 days or more), BMI (≤30 and >30 kg/m^{-2}), sex (male and female), viral load (≤5 and >5 copies/mL), and CRP (<39 mg/dL). Dispersion graphics were generated to represent the correlation between the selected proteins and age, viral load, BMI, and continuous variables comparing patients with mild versus moderate/severe COVID-19.

All statistical analyses were performed in R 4.2.2 [39], and a two-tailed p value <0.05 was considered significant.

Results

Baseline characteristics

The median age was higher for patients with moderate/severe (52 years) compared with mild (36 years) COVID-19. Time from symptom onset, viral load, and CRP levels were also higher in patients with moderate/severe COVID-19 than those with mild disease ($p = 0.002$, $p = 0.004$, and $p < 0.001$, respectively) (Table 1).

EV characterization

A total of 44 samples (one from each patient) collected at hospital admission were randomly read by NTA to measure the size (nm) and concentration of particles (particles/mL). The particle concentration and diameter did not differ between mild and moderate/severe COVID-19 in either of the two fractions analyzed (Student's *t*-test, $p > 0.05$) (Figure 2A). The structure of enriched EVs was observed by cryo-EM. A qualitative analysis showed that the EVs were intact after separation, with smooth surfaces and no clear internal density. EVs had membrane bilayers and some were multilayered (Figure 2B).

Proteomic data analysis

The relative quantification of the EV proteome was performed using the LFQ method. A total of 414 proteins were identified and quantified after excluding reverse sequences and identified only by the site (n = 14 from mild COVID-19 and n = 30 from moderate/severe COVID-19) (Supplementary Tables 1–4). A Venn diagram showed that 360 proteins were shared between both groups, and 6 proteins were observed exclusively in the mild group and 48 proteins in the moderate/severe group (Figure 3A). Unsupervised hierarchical clustering analysis using the Spearman distance with Ward linkage (Figure 3B) showed that two patients did not cluster perfectly to severity groups.

Enrichment analysis was performed using the protein-coding gene identifiers IDs (HUGO gene nomenclature). Analysis was performed for each of the two main protein clusters (PC1 = 234, PC2 = 180) separately in Gene Ontology (GO), and the top 10

TABLE 1
Characteristics of patients with mild and moderate/severe COVID-19 and SARS-CoV-2-positive by RT-PCR.

Characteristics	All patients (n = 44)		Mild (n = 14)		Moderate/severe (n = 30)		*p* value between groups
	n (%)	95% CI	n (%)	95% CI	n (%)	95% CI	
Age range, n (%)							
18–40 years	13 (30)	18–44	9 (64)	39–84	4 (13)	5–30	
41–59 years	19 (43)	30–58	5 (36)	16–61	14 (47)	30–64	<0.001
≥60 years	12 (27)	16–42	0 (0)	0–22	12 (40)	25–58	
Age (years), median (IQR)	49 (36–61)	42–52	36 (31–43)	28–47	52 (46–69)	48–65	<0.001
Sex, n (%)							
Female	18 (41)	28–56	9 (64)	39–84	9 (30)	17–48	0.068
Male	26 (59)	44–72	5 (36)	16–61	21 (70)	52–83	
Time from symptom onset, n (%)							
0–5 days	27 (61)	47–74	14 (100)	78–100	13 (43)	27–61	
6–10 days	13 (30)	18–44	0 (0)	0–22	13 (43)	27–61	0.002
≥11 days	4 (9)	4–21	0 (0)	0–22	4 (13)	5–30	
BMI, n (%)							
<30 kg/m^2	31(70)	56–82	10 (71)	45–88	21 (70)	52–83	1
≥30 kg/m^2	13 (30)	18–44	4 (29)	12–55	9 (30)	17–48	
Viral load, n (%)							
<5	29 (66)	51–78	14 (100)	78–100	15 (50)	33–67	
≥5	15 (34)	22–49	0 (0)	0–22	15 (50)	33–67	0.004
RT-PCR viral load (log_{10} copies/mL) median (IQR)	2.89 (2.46–6.35)	2.59–3.40	2.76 (2.49–3.32)	2.07–3.39	4.31 (2.42–7.15)	2.55–6.75	0.197
C-reactive protein (mg/L), median (IQR)	39.0 (10.8–103.3)	18.0–89.0	4.0 (1.5–10.8)	1.0–14.0	89.5 (42.8–115.8)	45.0–112.0	<0.001

Nontreated patients with mild and moderate/severe COVID-19 were included. RT-PCR, reverse transcriptase polymerase chain reaction; CI, confidence interval; IQR, interquartile range; BMI: body mass index. The chi-squared test was used for qualitative variables. The Mann-Whitney *U* test was used for between-group comparisons.

processes of each PC are depicted in Figure 3C. For PC1, the top five enriched processes were platelet degranulation (GO, 0002576; adjusted *p* value, 4.74E−32), exocytosis (GO, 0045055; adjusted *p* value, 5.44E−25), complement activation (GO, 0030449; adjusted *p* value, 8.12E−17), immune effector process (GO, 0002697; adjusted *p* value, 3.80E−15), and humoral immune response (GO, 0002920; adjusted *p* value, 5.42E−16) (Supplementary Table 5). For PC2, the top five enriched processes were neutrophil-mediated immunity (GO, 0002446; adjusted *p* value, 5.16E+03), high-density lipoprotein particle remodeling (GO, 0034375; adjusted *p* value, 5.16E+03), neutrophil degranulation (GO, 0043312; adjusted *p* value, 1.28E+05), neutrophil activation (GO, 0002283; adjusted *p* value, 1.28E+05), and triglyceride-rich lipoprotein particle remodeling (GO, 0034370; adjusted *p* value, 1.20E+07) (see Supplementary Table 6).

Selection of differentially abundant proteins by multivariate analysis

A total of 5 proteins were identified by multivariate analysis and considered relevant in the differentiation between mild and moderate/severe COVID-19 (Figure 4A): von Willebrand factor (PID, P04275), serum amyloid A-2 protein (PID, P0DJI9), histone H4 (PID, P62805), histone H2A type 2-C (PID, Q16777), and fibrinogen β-chain (PID, P02675). Among these, the von Willebrand factor was the most relevant to differentiate the cohorts because it had the highest regression coefficient (Figure 4B). Cross-validation of the model showed an accuracy of 95% (Figure 4C). An area under the curve (AUC) >0.92 was observed for each of the 5 proteins deemed differentially expressed in EVs from mild versus moderate/severe COVID-19 (Figure 4D). The abundance of all 5 proteins was greater in moderate/severe COVID-19 compared to the mild group, as shown in Figure 4E.

Figure 5 shows the association between abundance differences in the 5 proteins that are differentially present in mild versus moderate/severe COVID-19 and demographic and clinical characteristics. Among patients aged 41–59 years, the abundance differences of histone H4 was 527.2% higher in samples from the moderate/severe group than in samples from the mild group. Among female patients, the abundance differences of this protein in samples from the moderate/severe group was also 539.7% higher than in samples from the mild group. Furthermore, among samples from patients with BMI ≥30 kg/m^2, the histone H2A type 2-C showed abundance differences between the moderate/severe and mild groups of 392.9%.

Using Spearman correlations we found that levels of von Willebrand factor, serum amyloid A-2, histones H4 and H2A type 2-C, as well as fibrinogen β-chain were positively correlated with age, viral load, and CRP levels, but not with BMI (Figure 6).

Discussion

In this exploratory secondary analysis of samples collected from two RCTs (control arm) [28,29], we found that serum-derived EVs from patients with COVID-19 may be a valuable source of information regarding disease severity. Although we found no differences in particle concentration and diameter, EV proteome was different between mild and moderate/severe cases, indicating that EV content can be altered in response to SARS-CoV-2 infection. Moreover, the nature of the proteins contained in these EVs and the abundance differences associated with severity provide biological plausibility for their involvement in disease pathogenesis and progression.

Proteomic analysis revealed abundance differences of various proteins related to immune responses, activation of coagulation, and complement pathways in more severe cases of COVID-19, confirming data from other studies [25–27], which suggest that serum-derived EVs may play an essential role in tissue injury and multiple organ involvement. Five key proteins (von Willebrand factor, serum amyloid A-2, histones H4 and H2A type 2-C, and fibrinogen β-chain) were observed to be differentially abundant in EVs from mild versus moderate/severe COVID-19 patients. In addition to potentially functioning as future biomarkers of disease severity, their known function in the activation of pivotal signaling pathways associated with inflammation and hypercoagulability suggests they may be explored as biotargets for therapy.

Previous studies have recognized the potential utility of EVs as biomarkers that reflect the pathologic state of several diseases [21–24], and recent studies have demonstrated that EV cargo can also be used to differentiate severity in patients with COVID-19 [25–27]. In comparison to previous studies, we used herein a study design that capitalizes on samples collected in the context of RCTs [28,29] – where patient heterogeneity was minimized by the application of strict inclusion/exclusion criteria and randomization, bias was reduced by blinding, and trained research coordinators and

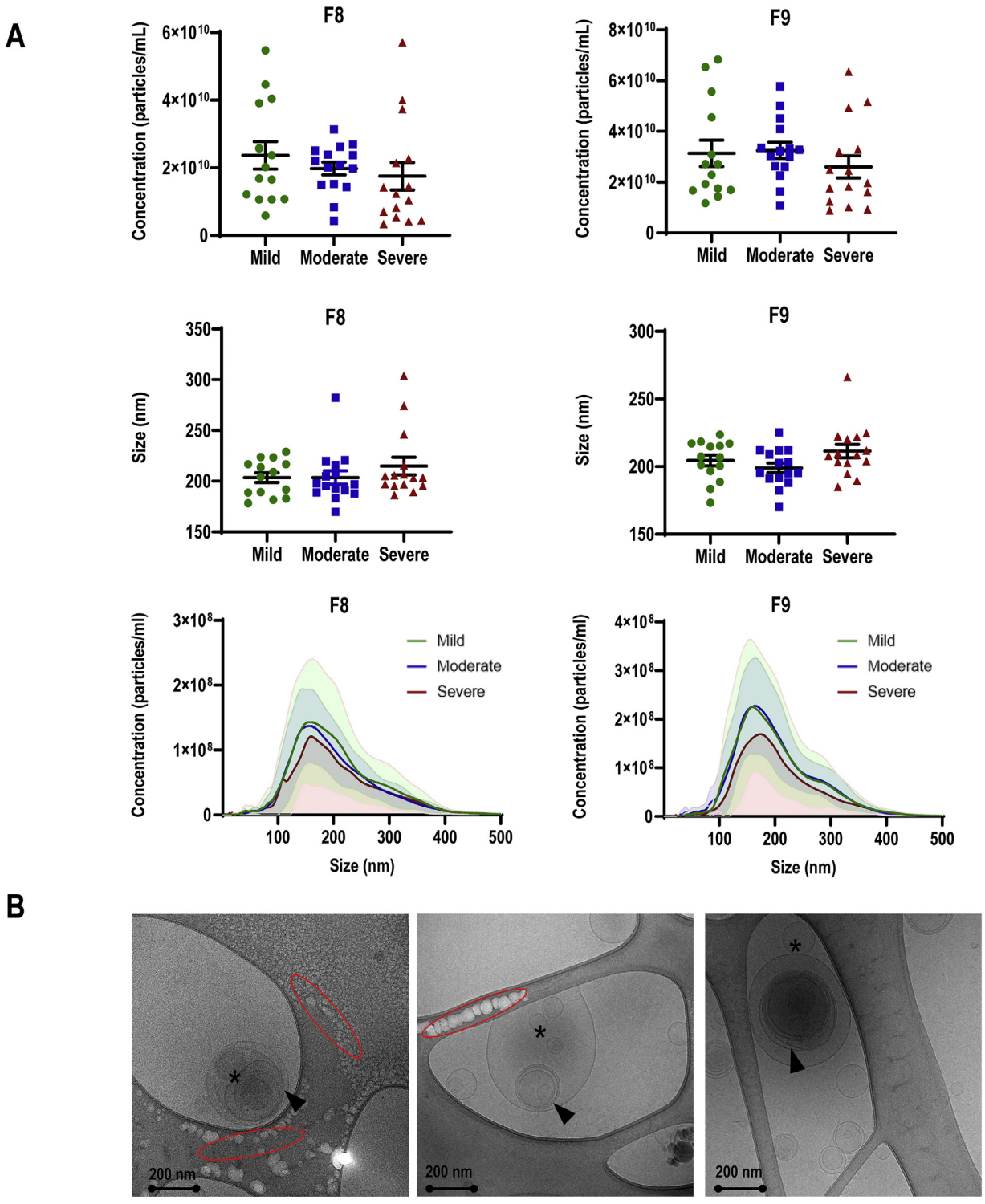

FIGURE 2. Characterization of extracellular vesicles (EVs) separated and enriched from patients with mild and moderate/severe COVID-19. (A) The particle concentration and diameter, measured in fractions 8 and 9, are presented as the mean and standard error of the mean. No statistically significant differences were found between the groups regarding the particle concentration and diameter. Nanoparticle concentration as a function of the size distribution of mild (green) and moderate/severe (red) samples measured by nanoparticle tracking analysis. Values are means ± standard deviation, n = 14 measurements (mild) and n = 30 measurements (moderate/severe). (B) Representative cryo-electron microscopy image of EVs from patients with mild (left), moderate (central), and severe (right) COVID-19. EVs had membrane bilayers (arrows) and some were multilayered. No qualitative differences were observed between the structures of the EVs, since we included NTA data that provide a more reliable measure of particle concentration and diameter. The white structures on the carbon film are bubbles that appear when a hydrated biological sample is under prolonged exposure to the electron beam (indicated by red solid ellipse). Asterisks: smaller vesicular structures.

laboratory technician who used standard operating procedures for collection, handling, and storage of samples, thus optimizing both internal and external validity of molecular findings and minimizing batch effect. Altogether, these features maximize the potential for the identification of more robust EV-derived protein biomarkers associated with the phenotypes of interest.

Because serum from patients with COVID-19 represents a relevant biofluid collected minimally invasively that recapitulates alterations

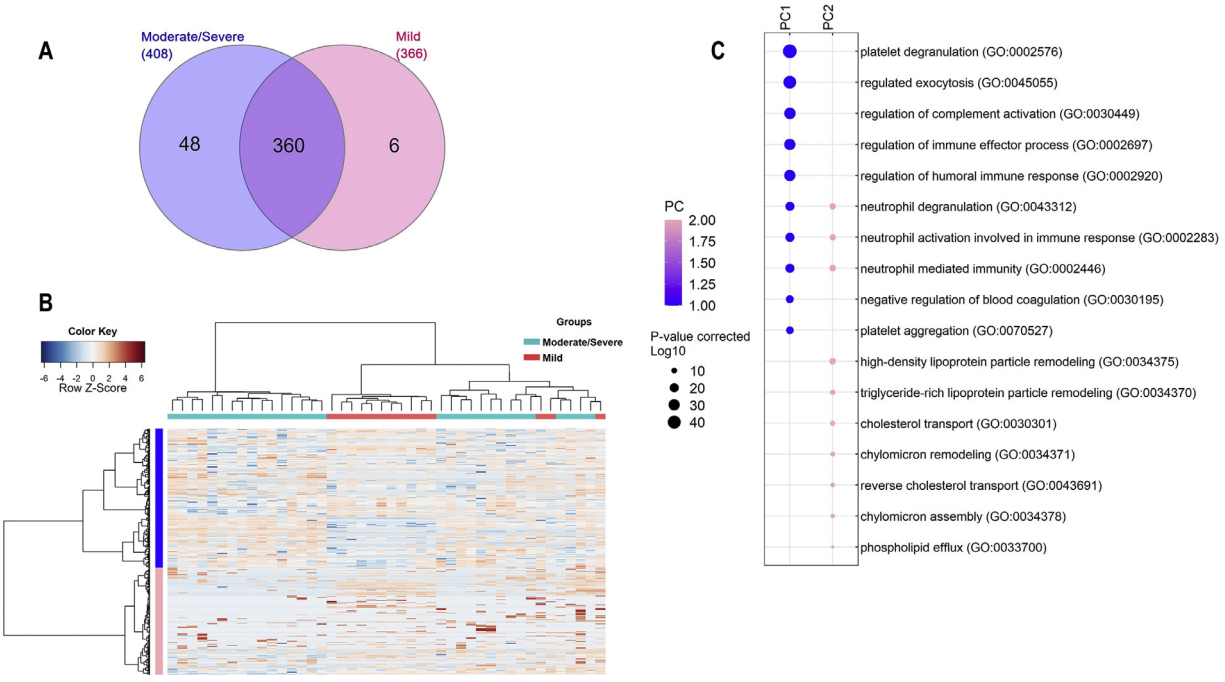

FIGURE 3. Proteomic profile of extracellular vesicles (EVs) from patients with mild versus moderate/severe COVID-19. (A) Venn diagram of common and exclusive proteins identified for patients with mild and moderate/severe COVID-19. (B) Hierarchical clustering analysis of proteins identified in the mild group (n = 14 samples) and the moderate/severe group (n = 30 samples). Values for each protein (rows) and each EV sample (columns) are colored based on the protein abundance; high (red) and low (blue) values (Z-scored log2 label-free quantification intensity values) are indicated based on the color scale bar shown at the top left of the figure. The colored bars shown at the top of the figure indicate the severe and moderate samples (blue) or mild samples (pink). Hierarchical clustering was performed in the R environment using the Spearman distance with Ward linkage. (C) Top 10 significant Gene Ontology biological processes enriched for the proteins cluster groups (PC1 and PC2) of the global proteome (adjusted p value ≤ 0.05; two-sided Fisher's exact test followed by Benjamini-Hochberg correction).

throughout the body [40,41], we used these samples to then purify EVs for subsequent analysis. Although criteria for characterization and studies of EVs have been defined [19], there is no gold standard method for EV separation; therefore, we selected an established protocol associated with an SEC-based approach for enrichment of the EVs. Even though it is not possible to fully eliminate the presence of potential contamination of non-EV proteins, this method enables the use of small volumes of serum, which is a common need for experiments assessing clinical samples [30–33].

We used the GLM with LASSO regression because it has been shown to be a powerful method for protein selection and disease prediction, thus leading to reduced dimensionality and sparsity, common problems when we have more factors than patients. This methodology has previously been used to predict graft-versus-host disease. In that approach, random tree models were used to identify markers for classifying disease; the GLM was more effective in the selection of the most promising hits, reducing the panel of 785 detected proteins to 13 discriminant markers with significant diagnostic accuracy [42]. In a dataset with small volume samples, the GLM was also effective for protein selection in Alzheimer's disease prediction with an acceptable AUC approaching 70% using cerebrospinal fluid and 90% using plasma [43]. By using the GLM for bioinformatics analysis, our proteomic data revealed an enrichment of proteins related to platelet degranulation, exocytosis, complement activation, immune effector activation, and humoral immune response in more severe cases of COVID-19. Interestingly, neutrophil degranulation and activation were also identified as relevant biological processes in the enrichment analysis of proteins from serum-derived EVs, regardless of COVID-19 severity. These results point to an essential role for neutrophils in COVID-19 development, which corresponds to clinical findings [3,13,44,45].

Platelet degranulation was the most enriched biological process in our investigation with serum-derived EVs from patients with moderate/severe COVID-19. This finding is in line with previous publications [27,46,47], indicating increased formation of platelet and platelet-leukocyte aggregates in more severe cases of COVID-19 and contributing to worse disease prognosis. During the initial phase of SARS-CoV-2 infection, circulating platelets become hyperresponsive to agonist stimulation and exhibit increased expression of surface markers [48], leading to hyperactivation and aggregation of platelets that contribute to the hypercoagulable state of severe COVID-19 [47]. The increased formation of platelet aggregates in more severe cases of COVID-19 has also been correlated to increased levels of CRP and interleukin-6 [49,50]. In this context, we also identified abundance differences of fibrinogen β-chain in serum-derived EVs from patients with moderate/severe COVID-19 compared to those with mild disease. Besides fibrinogen β-chain, increased values of fibrinogen α-chain and γ-chain have also been reported in previous COVID-19 cases [25]. These clotting factors can present increased levels during SARS-CoV-2-mediated inflammatory responses, promoting alterations in the coagulation process that lead to the formation of thrombi [51]. Moreover, increased fibrinogen levels have been associated with elevated D-dimer values, more severe phenotypes, and the need for intensive care [52]. In autopsy studies of COVID-19, fibrin-rich thrombi were also found in small vessels and pulmonary capillaries [53]. Fibrinogen levels were shown to be altered in plasma and saliva from convalescent patients, highlighting a potential role of these factors in the post-COVID syndrome [54]. Our data also demonstrated abundance differences of von Willebrand factor in patients with moderate/severe COVID-19 compared with mild cases. This soluble protein is secreted by platelets during endothelial cell injury and the formation of thrombi [55] and participates in SARS-CoV-2-mediated pathologic mechanisms by triggering the thrombo-inflammatory complications that are commonly observed in cases of severe COVID-19 [3–5].

Tissue factor (also termed coagulation factor III) is another major component of the coagulation cascade that is upregulated in COVID-19 [56]. Its expression can be increased by complement factors,

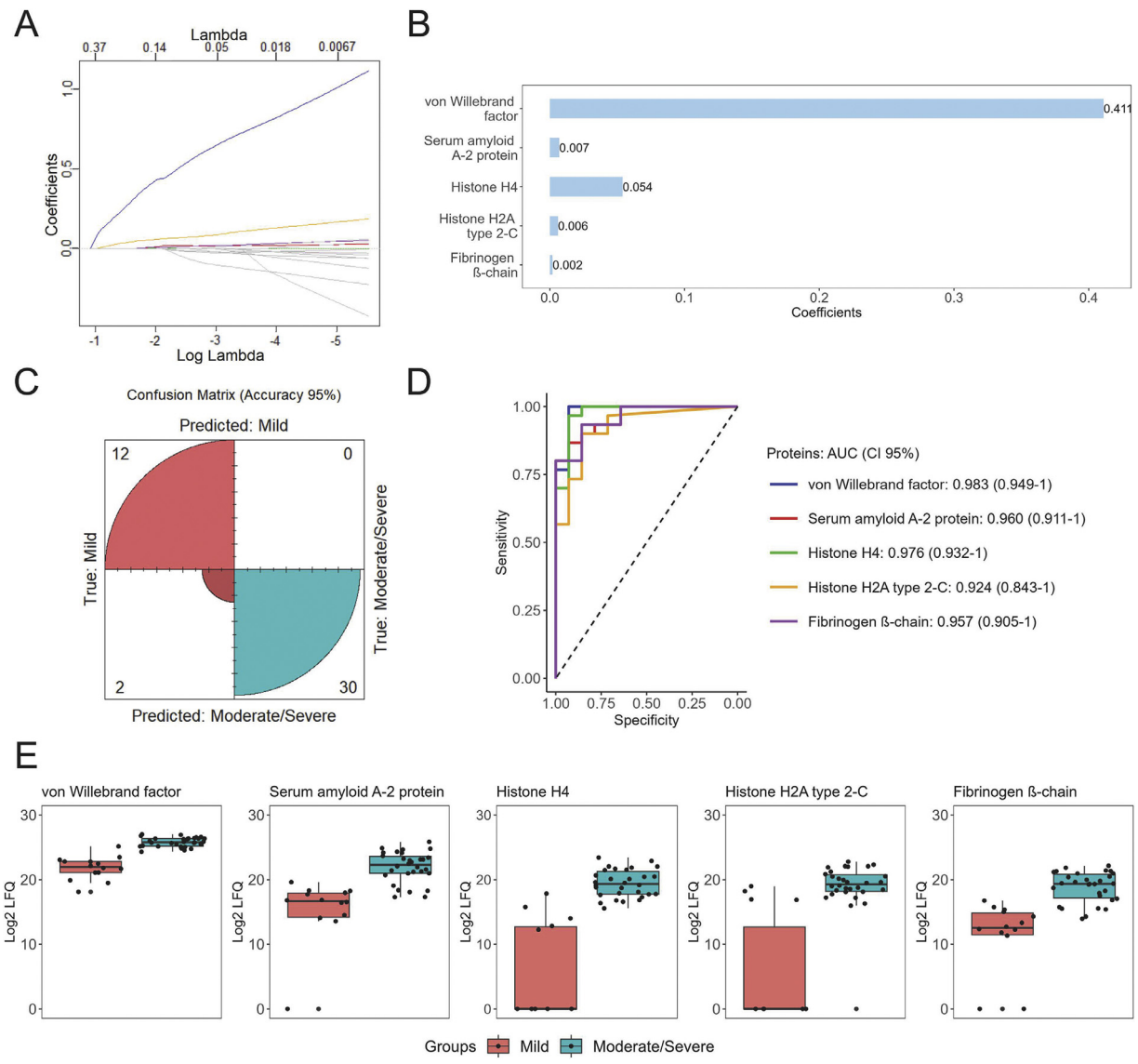

FIGURE 4. Multivariate analysis identification of differences in EV protein abundance. (A) Coefficients of all proteins included in the LASSO regression model against lambda values. The closer the coefficient is to zero, the less representative the protein is in the differentiation between mild and moderate/severe. (B) Bar graph of proteins with coefficients different from 0 selected in LASSO regression. The magnitude of the coefficients indicates the degree of importance of the protein in the differentiation between mild and moderate/severe. (C) A confusion matrix for validating the predictive ability of selected proteins. True moderate/severe patients are shown in blue, and truly mild patients in pink. The accuracy was 95%. (D) Receiver operating characteristic area under the curve (AUC) from validation of selected proteins. (E) Boxplot graph of selected proteins according to the mild and moderate/severe classification. CI, confidence interval.

leading to thrombin activation and increased formation of platelet aggregates [56]. In this context, our proteomic data identified enrichment for complement activation in serum-derived EVs from patients with moderate/severe COVID-19. Although the complement system plays an important role in favoring clearance during viral infection, its dysregulated activation and propagation stimulate the coagulation pathway and promote extensive tissue injury [57]. In line with our findings, previous studies have reported dysregulation of the complement system [11,27,58,59] with altered expression of transcription factors associated with complement activation in SARS-CoV-2 infection [25,60]. Increased plasma levels of complement factors and their deposition in the lungs were also observed in severely ill patients hospitalized with COVID-19 [61,62], reinforcing the dysregulation of the complement system as a hallmark in the hypercoagulable state in more severe cases.

At the onset of infection, the immune system is activated to protect the body and eliminate pathogens, such as SARS-CoV-2; however, excessive activation becomes harmful to the host because it can cause the release of intracellular components into the extracellular space to neutralize the pathogen but that also promotes further inflammation and tissue injury [63–65]. Our analysis identified abundance differences of histones H2A type 2-C and H4 in circulating EVs from moderate/severe COVID-19 cases compared with mild cases. These nuclear proteins provide structural and functional support to condensate the DNA into chromosomes under normal physiological conditions [64,65]; however, upon apoptosis/necrosis (an unregulated process) or formation of neutrophil extracellular traps (NETs) (a regulated process), they are released into the extracellular space and function as damage-associated molecular patterns that promote cell activation [66], Toll-like receptor (TLR)-mediated immune responses [65,67], and cell death [68]. In particular, histone H4 can directly bind to TLR4 on the cell surface of peripheral blood-derived monocytes, leading to the release of chemokines and, consequently, increased recruitment of inflammatory cells [65,67]. Previous studies have demonstrated increased levels of histones and other NET

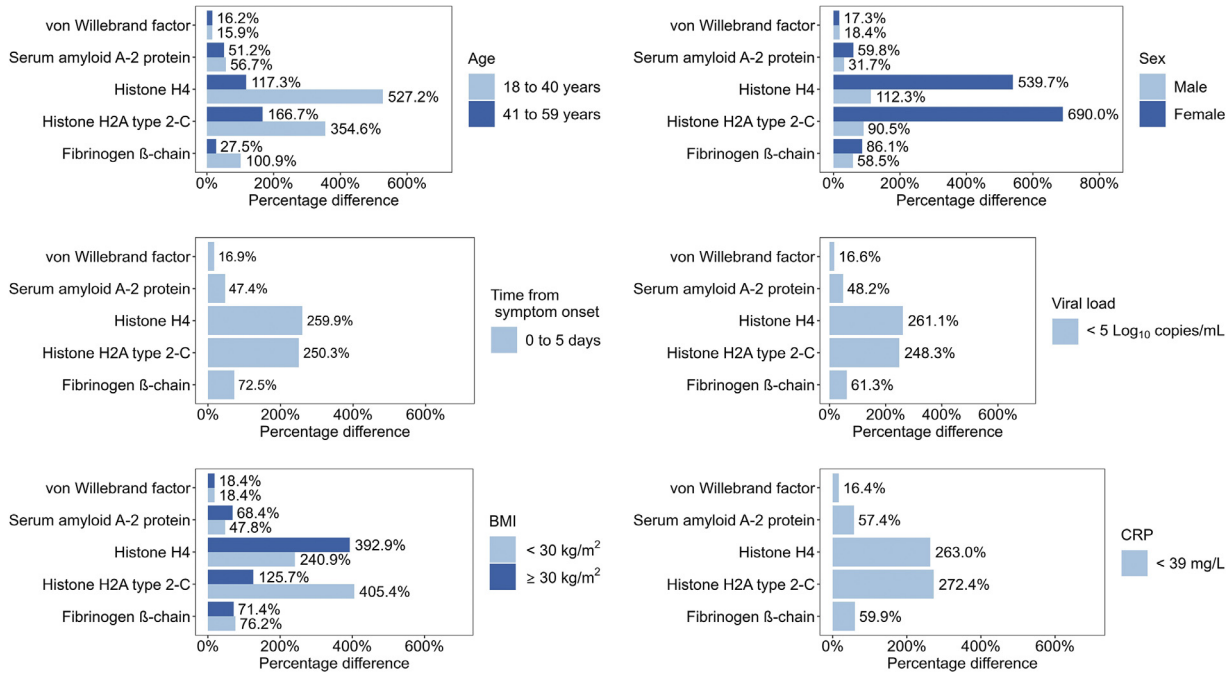

FIGURE 5. Abundance differences in proteins between the mild and moderate/severe group for each clinical variable calculated by (mild−moderate/severe)/mild × 100. BMI, body mass index; CRP, C-reactive protein.

components in patients with COVID-19 [69–71] that directly correlate to disease severity [70,72], which is in line with our findings. Moreover, histones have a major role not only in SARS-CoV-2-mediated inflammation but also in hypercoagulation. A significant increase in tissue factor activity and thrombin generation by peripheral blood-derived monocytes has been observed in the presence of extracellular histones [73,74]. NET components have also been associated with deposited platelets and microthrombi formation in the lungs of patients with COVID-19 [75]. Quantitative assessment of histone-DNA complex in samples from patients with COVID-19 has been shown to have prognostic value in discriminating disease severity [76–78].

Patients with COVID-19 can present a hyperinflammatory state with increased levels of numerous proteins associated with leukocyte recruitment and immune response activation (also termed cytokine storm), which participate in dysregulated immune responses and worsening of clinical outcomes [3,5,25]. Our analysis identified serum amyloid A2 (SAA2) as a key protein in serum-derived EVs, which demonstrated abundance differences between moderate/severe cases and mild cases of COVID-19. This biomarker, produced in the liver, is activated during the acute phase response of inflammatory and infective processes, promoting strong chemoattractant activity even at low levels [79]. Increased levels of circulating SAA2 are associated with chest CT scan findings and correlate to poor prognosis in COVID-19 [80] with even greater levels of this protein observed in patients who required intensive care compared with those who did not [11]. The SAA2 isoforms (SAA1, SAA3, and SAA4) are also increased in more severe cases [11,25,41], demonstrating the relevance of these proteins for the prognosis of COVID-19. Previous results have demonstrated that SAA levels significantly decreased in hospitalized patients with COVID-19 who recovered well and were discharged, whereas these levels continued to be elevated in patients who died or worsened [80,81].

Advanced age, obesity, high viral load, and long virus-shedding period have been associated with worse prognosis in COVID-19 [1,82–84]. Even though the levels of the top five proteins (von Willebrand factor, serum amyloid A-2, fibrinogen β-chain, and histones H4 and H2A type 2-C) identified in our data were not correlated with BMI, they strongly correlated with age, viral load, and CRP levels, providing further evidence of their relevance as biomarkers associated with COVID-19 severity.

Some limitations in our study should be considered. Firstly, a small number of samples from each cohort was assessed. It is known that serum proteomic studies have small sample sizes, which may be attributed to (i) difficulties in sourcing serum samples with sufficient quality and (ii) high sample processing costs. This is an exploratory secondary analysis of two RCTs, which presents less heterogeneity, thus allowing for fewer samples [28,29]. Our results provide unique and experimentally novel insights that hopefully will lead to innovative hypotheses moving forward. Secondly, samples were collected at a single time point, which was at the moment of admission. This occurred 4–5 days after symptom onset in mild COVID-19 and 5–10 days in moderate/severe COVID-19 cases. The third limitation concerns longitudinal analysis since patients from both RCTs were followed up for only 14 days, after which no data were collected. Finally, mechanistic validation of the most relevant markers should be further investigated in future studies. Additionally, more robust analyses on discovery and validation samples are required.

Conclusions

Using samples collected within the framework of two RCTs, we have demonstrated that EV content is significantly altered in COVID-19 across the spectrum of severity. Our experimental design is exploratory and did not allow for longitudinal sample analysis, but it is feasible that monitoring EV cargo from patients with COVID-19 may provide valuable information for the prediction of disease severity. Combined information about risk factors and protein biomarkers identified herein may be a more informative strategy to monitor the severity and potential outcomes of COVID-19 than clinical and biochemical markers alone.

Declaration of competing interest

All authors declare no actual or potential conflict of interest including any financial, personal or other relationships with other

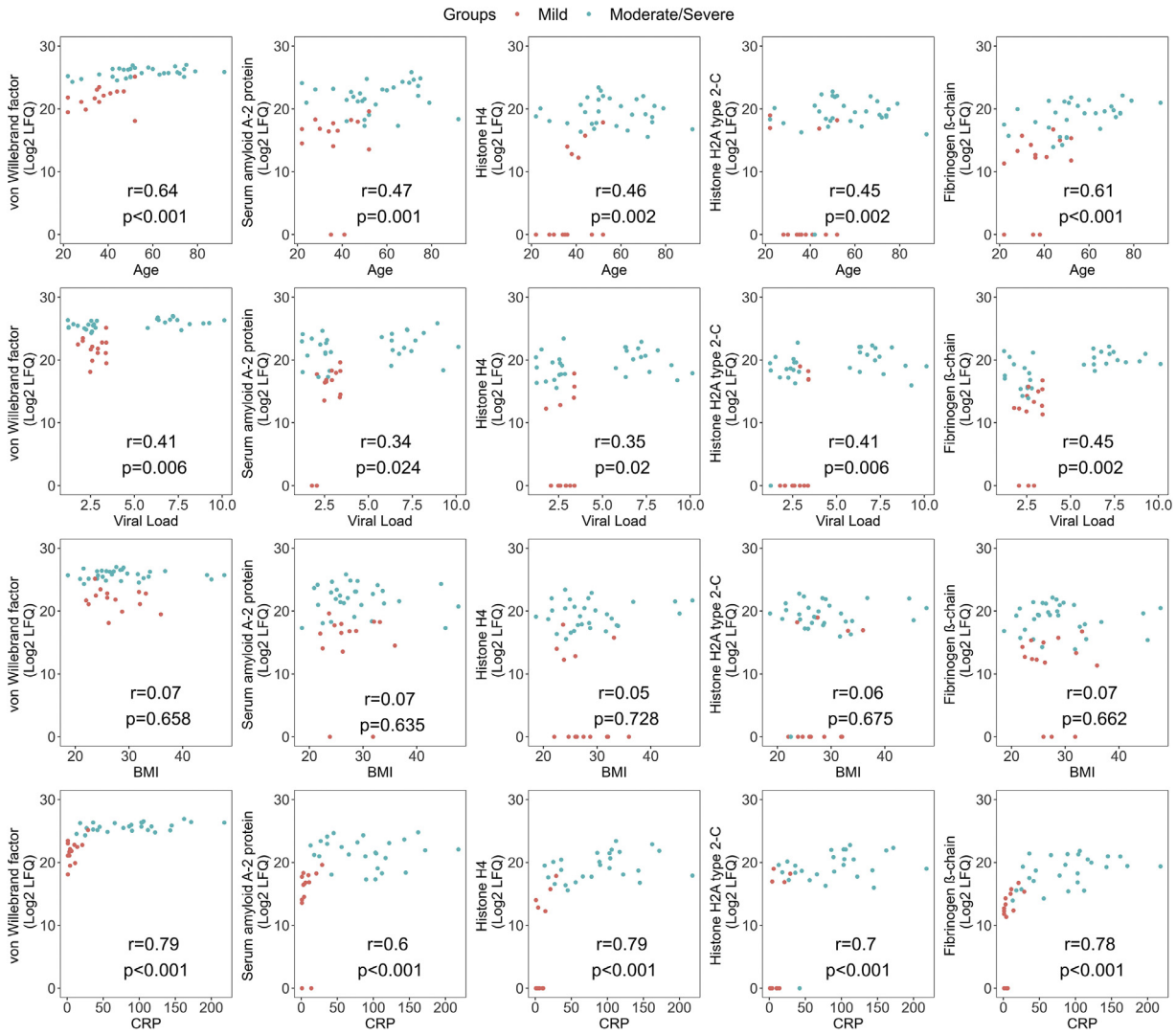

FIGURE 6. Correlation between selected proteins and age, viral load, body mass index (BMI), and C-reactive protein (CRP) according to the mild and moderate/severe groups. r, Spearman correlation coefficient.

people or organizations within three (3) years of beginning the work submitted that could inappropriately influence (bias) their work.

Funding

This work was supported by the Brazilian Council for Scientific and Technological Development (CNPq), Brazil (number: 403485/2020-7 [PRMR], 310392/2021-7 [AFLP]), Funding Authority for Studies and Projects (FINEP), Brasília, Brazil (number: 01.20.0003.00), FAPESP (numbers 2009/54067- 3 [AFPL], 2018/18496-6 [AFPL], 2019/09692-9 [AGCN], and 20/11709-4 [JVO]), and the Rio de Janeiro State Research Foundation (COVID-19- FAPERJ) E-26/210.181/2020 [PRMR]. This work was also partially supported by/or received resources from the Brazilian Federal Government provided to the Center for Research in Energy and Materials (CNPEM), a private nonprofit organization under the supervision of the Brazilian Ministry for Science, Technology, and Innovation (MCTI). The proteomic analysis was performed at the Mass Spectrometry Laboratory of the Brazilian Biosciences National Laboratory (LNBio), which is part of CNPEM.

Acknowledgments

The Mass Spectrometry Laboratory staff are acknowledged for their assistance during the experiments. The authors would like to thank LNNano/CNPEM for the access to the electron microscopy facility. We would like to thank Moira Elizabeth Shottler, mBA, Rio de Janeiro, Brazil, and Lorna O'Brien (authorserv.com) for editing assistance.

Author Contributions

Conception and design of the study: AFPL and PRMR. Acquisition of data: Acquisition of data: AFPL, SY, AGCN, JVSO, RRD. Analysis and interpretation of data: AFPL, FFC, PLS, BSFS, CCS, HCFN, CMM, PRMR Drafting or revising the manuscript: AFPL, MLP, PRMR. All authors have approved the final article.

Supplementary materials

Supplementary material associated with this article can be found in the online version at doi:10.1016/j.jcyt.2024.02.001.

References

[1] Williamson EJ, Walker AJ, Bhaskaran K, Bacon S, Bates C, Morton CE, et al. Factors associated with COVID-19-related death using OpenSAFELY. Nature 2020;584:430–6. https://doi.org/10.1038/s41586-020-2521-4.

[2] World Health Organization. WHO coronavirus (COVID-19) dashboard n.d. https://covid19.who.int/ [accessed 08.08.23].

[3] Huang C, Wang Y, Li X, Ren L, Zhao J, Hu Y, et al. Clinical features of patients infected with 2019 novel coronavirus in Wuhan, China. Lancet 2020;395:497–506. https://doi.org/10.1016/S0140-6736(20)30183-5.
[4] Klok FA, Kruip MJHA, van der Meer NJM, Arbous MS, Gommers DAMPJ, Kant KM, et al. Incidence of thrombotic complications in critically ill ICU patients with COVID-19. Thromb Res 2020;191:145–7. https://doi.org/10.1016/j.thromres.2020.04.013.
[5] Lopes-Pacheco M, Silva PL, Cruz FF, Battaglini D, Robba C, Pelosi P, et al. Pathogenesis of multiple organ injury in COVID-19 and potential therapeutic strategies. Front Physiol 2021;12:593223. https://doi.org/10.3389/fphys.2021.593223.
[6] Robba C, Battaglini D, Pelosi P, Rocco PRM. Multiple organ dysfunction in SARS-CoV-2: MODS-CoV-2. Expert Rev Respir Med 2020;14:865–8. https://doi.org/10.1080/17476348.2020.1778470.
[7] Hodgson CL, Higgins AM, Bailey MJ, Mather AM, Beach L, Bellomo R, et al. The impact of COVID-19 critical illness on new disability, functional outcomes and return to work at 6 months: a prospective cohort study. Crit Care 2021;25:382. https://doi.org/10.1186/s13054-021-03794-0.
[8] Gil S, Gualano B, de Araújo AL, de Oliveira Júnior GN, Damiano RF, Pinna F, et al. Post-acute sequelae of SARS-CoV-2 associates with physical inactivity in a cohort of COVID-19 survivors. Sci Rep 2023;13:215. https://doi.org/10.1038/s41598-022-26888-3.
[9] Halawa S, Pullamsetti SS, Bangham CRM, Stenmark KR, Dorfmüller P, Frid MG, et al. Potential long-term effects of SARS-CoV-2 infection on the pulmonary vasculature: a global perspective. Nat Rev Cardiol 2022;19:314–31. https://doi.org/10.1038/s41569-021-00640-2.
[10] Ning Q, Wu D, Wang X, Xi D, Chen T, Chen G, et al. The mechanism underlying extrapulmonary complications of the coronavirus disease 2019 and its therapeutic implication. Signal Transduct Target Ther 2022;7:57. https://doi.org/10.1038/s41392-022-00907-1.
[11] Ciccosanti F, Antonioli M, Sacchi A, Notari S, Farina A, Beccacece A, et al. Proteomic analysis identifies a signature of disease severity in the plasma of COVID-19 pneumonia patients associated to neutrophil, platelet and complement activation. Clin Proteomics 2022;19:38. https://doi.org/10.1186/s12014-022-09377-7.
[12] Cosgriff C V, Miano TA, Mathew D, Huang AC, Giannini HM, Kuri-Cervantes L, et al. Validating a proteomic signature of severe COVID-19. Crit Care Explor 2022;4:e0800. https://doi.org/10.1097/CCE.0000000000000800.
[13] Battaglini D, Lopes-Pacheco M, Castro-Faria-Neto HC, Pelosi P, Rocco PRM. Laboratory biomarkers for diagnosis and prognosis in COVID-19. Front Immunol 2022;13:857573. https://doi.org/10.3389/fimmu.2022.857573.
[14] Leisman DE, Ronner L, Pinotti R, Taylor MD, Sinha P, Calfee CS, et al. Cytokine elevation in severe and critical COVID-19: a rapid systematic review, meta-analysis, and comparison with other inflammatory syndromes. Lancet Respir Med 2020;8:1233–44. https://doi.org/10.1016/S2213-2600(20)30404-5.
[15] Abreu SC, Lopes-Pacheco M, Weiss DJ, Rocco PRM. Mesenchymal stromal cell-derived extracellular vesicles in lung diseases: current status and perspectives. Front Cell Dev Biol 2021;9:600711. https://doi.org/10.3389/fcell.2021.600711.
[16] da Silva KN, Gobatto ALN, Costa-Ferro ZSM, Cavalcante BRR, Caria ACI, de Aragão França LS, et al. Is there a place for mesenchymal stromal cell-based therapies in the therapeutic armamentarium against COVID-19? Stem Cell Res Ther 2021;12:425. https://doi.org/10.1186/s13287-021-02502-7.
[17] dos Santos CC, Lopes-Pacheco M, English K, Rolandsson Enes S, Krasnodembskaya A, Rocco PRM. The MSC-EV-microRNAome: a perspective on therapeutic mechanisms of action in sepsis and ARDS. Cells 2024;13:122. https://doi.org/10.3390/cells13020122.
[18] Yáñez-Mó M, Siljander PR-M, Andreu Z, Zavec AB, Borràs FE, Buzas EI, et al. Biological properties of extracellular vesicles and their physiological functions. J Extracell Vesicles 2015;4:27066. https://doi.org/10.3402/jev.v4.27066.
[19] Théry C, Witwer KW, Aikawa E, Alcaraz MJ, Anderson JD, Andriantsitohaina R, et al. Minimal information for studies of extracellular vesicles 2018 (MISEV2018): a position statement of the International Society for Extracellular Vesicles and update of the MISEV2014 guidelines. J Extracell Vesicles 2018;7:1535750. https://doi.org/10.1080/20013078.2018.1535750.
[20] Mathieu M, Martin-Jaular L, Lavieu G, Théry C. Specificities of secretion and uptake of exosomes and other extracellular vesicles for cell-to-cell communication. Nat Cell Biol 2019;21:9–17. https://doi.org/10.1038/s41556-018-0250-9.
[21] Ax E, Jevnikar Z, Cvjetkovic A, Malmhäll C, Olsson H, Rådinger M, et al. T2 and T17 cytokines alter the cargo and function of airway epithelium-derived extracellular vesicles. Respir Res 2020;21:155. https://doi.org/10.1186/s12931-020-01402-3.
[22] Novikova SE, Soloveva NA, Farafonova TE, Tikhonova O V, Liao P-C, Zgoda VG. Proteomic signature of extracellular vesicles for lung cancer recognition. Molecules 2021;26:6145–64. https://doi.org/10.3390/molecules26206145.
[23] Koba T, Takeda Y, Narumi R, Shiromizu T, Nojima Y, Ito M, et al. Proteomics of serum extracellular vesicles identifies a novel COPD biomarker, fibulin-3 from elastic fibres. ERJ Open Res 2021;7:00658–2020. https://doi.org/10.1183/23120541.00658-2020.
[24] Morris DC, Jaehne AK, Chopp M, Zhang Z, Poisson L, Chen Y, et al. Proteomic Profiles of exosomes of septic patients presenting to the emergency department compared to healthy controls. J Clin Med 2020;9:2930–43. https://doi.org/10.3390/jcm9092930.
[25] Barberis E, Vanella V V, Falasca M, Caneapero V, Cappellano G, Raineri D, et al. Circulating exosomes are strongly involved in SARS-CoV-2 infection. Front Mol Biosci 2021;8:632290. https://doi.org/10.3389/fmolb.2021.632290.
[26] Mao K, Tan Q, Ma Y, Wang S, Zhong H, Liao Y, et al. Proteomics of extracellular vesicles in plasma reveals the characteristics and residual traces of COVID-19 patients without underlying diseases after 3 months of recovery. Cell Death Dis 2021;12:541. https://doi.org/10.1038/s41419-021-03816-3.
[27] Moraes ECDS, Martins-Gonçalves R, da Silva LR, Mandacaru SC, Melo RM, Azevedo-Quintanilha I, et al. Proteomic Profile of procoagulant extracellular vesicles reflects complement system activation and platelet hyperreactivity of patients with severe COVID-19. Front Cell Infect Microbiol 2022;12:926352. https://doi.org/10.3389/fcimb.2022.926352.
[28] Rocco PRM, Silva PL, Cruz FF, Tierno PFGMM, Rabello E, Junior JC, et al. Nitazoxanide in patients hospitalized with COVID-19 pneumonia: a multicentre, randomized, double-blind, placebo-controlled trial. Front Med 2022;9:844728. https://doi.org/10.3389/fmed.2022.844728.
[29] Rocco PRM, Silva PL, Cruz FF, Melo-Junior MAC, Tierno PFGMM, Moura MA, et al. Early use of nitazoxanide in mild COVID-19 disease: randomised, placebo-controlled trial. Eur Respir J 2021;58:2003725–35. https://doi.org/10.1183/13993003.03725-2020.
[30] Vanderboom PM, Dasari S, Ruegsegger GN, Pataky MW, Lucien F, Heppelmann CJ, et al. A size-exclusion-based approach for purifying extracellular vesicles from human plasma. Cell Reports Methods 2021;1:100055–68. https://doi.org/10.1016/j.crmeth.2021.100055.
[31] Vinik Y, Ortega FG, Mills GB, Lu Y, Jurkowicz M, Halperin S, et al. Proteomic analysis of circulating extracellular vesicles identifies potential markers of breast cancer progression, recurrence, and response. Sci Adv 2020;6:eaba5714–5725. https://doi.org/10.1126/sciadv.aba5714.
[32] Veerman RE, Teeuwen L, Czarnewski P, Güclüler Akpinar G, Sandberg A, Cao X, et al. Molecular evaluation of five different isolation methods for extracellular vesicles reveals different clinical applicability and subcellular origin. J Extracell Vesicles 2021;10:e12128–12153. https://doi.org/10.1002/jev2.12128.
[33] Stranska R, Gysbrechts L, Wouters J, Vermeersch P, Bloch K, Dierickx D, et al. Comparison of membrane affinity-based method with size-exclusion chromatography for isolation of exosome-like vesicles from human plasma. J Transl Med 2018;16:1. https://doi.org/10.1186/s12967-017-1374-6.
[34] Busso-Lopes AF, Carnielli CM, Winck FV, Patroni FM de S, Oliveira AK, Granato DC, et al. A reductionist approach using primary and metastatic cell-derived extracellular vesicles reveals hub proteins associated with oral cancer prognosis. Mol Cell Proteomics 2021;20:100118. https://doi.org/10.1016/j.mcpro.2021.100118.
[35] Winck F V, Prado Ribeiro AC, Ramos Domingues R, Ling LY, Riaño-Pachón DM, Rivera C, et al. Insights into immune responses in oral cancer through proteomic analysis of saliva and salivary extracellular vesicles. Sci Rep 2015;5:16305. https://doi.org/10.1038/srep16305.
[36] Rappsilber J, Mann M, Ishihama Y. Protocol for micro-purification, enrichment, pre-fractionation and storage of peptides for proteomics using StageTips. Nat Protoc 2007;2:1896–906. https://doi.org/10.1038/nprot.2007.261.
[37] Perez-Riverol Y, Csordas A, Bai J, Bernal-Llinares M, Hewapathirana S, Kundu DJ, et al. The PRIDE database and related tools and resources in 2019: improving support for quantification data. Nucleic Acids Res 2019;47:D442–50. https://doi.org/10.1093/nar/gky1106.
[38] Kuhn MT, Hutchison JL, Norman HD. Modeling nuisance variables for prediction of service sire fertility. J Dairy Sci 2008;91:2823–35. https://doi.org/10.3168/jds.2007-0946.
[39] Team RC. R: a language and environment for statistical computing. R Found Stat Comput 2020 https://www.r-project.org/.
[40] Csősz É, Kalló G, Márkus B, Deák E, Csutak A, Tőzsér J. Quantitative body fluid proteomics in medicine: a focus on minimal invasiveness. J Proteomics 2017;153:30–43. https://doi.org/10.1016/j.jprot.2016.08.009.
[41] Pagani L, Chinello C, Risca G, Capitoli G, Criscuolo L, Lombardi A, et al. Plasma proteomic variables related to COVID-19 severity: an untargeted nLC-MS/MS investigation. Int J Mol Sci 2023;24:3570. https://doi.org/10.3390/ijms24043570.
[42] O'Leary OE, Schoetzau A, Amruthalingam L, Geber-Hollbach N, Plattner K, Jenoe P, et al. Tear proteomic predictive biomarker model for ocular graft versus host disease classification. Transl Vsion Sci Technol 2020;9(9):3–18. https://doi.org/10.1167/tvst.9.9.3.
[43] Whelan CD, Mattsson N, Nagle MW, Vijayaraghavan S, Hyde C, Janelidze S, et al. Multiplex proteomics identifies novel CSF and plasma biomarkers of early Alzheimer's disease. Acta Neuropathol Commun 2019;7:169. https://doi.org/10.1186/s40478-019-0795-2.
[44] Liu Y, Du X, Chen J, Jin Y, Peng L, Wang HHX, et al. Neutrophil-to-lymphocyte ratio as an independent risk factor for mortality in hospitalized patients with COVID-19. J Infect 2020;81:e6–12. https://doi.org/10.1016/j.jinf.2020.04.002.
[45] Käsine T, Dyrhol-Riise AM, Barratt-Due A, Kildal AB, Olsen IC, Nezvalova-Henriksen K, et al. Neutrophil count predicts clinical outcome in hospitalized COVID-19 patients: results from the NOR-Solidarity trial. J Intern Med 2022;291:241–3. https://doi.org/10.1111/joim.13377.
[46] Hottz ED, Azevedo-Quintanilha IG, Palhinha L, Teixeira L, Barreto EA, Pão CRR, et al. Platelet activation and platelet-monocyte aggregate formation trigger tissue factor expression in patients with severe COVID-19. Blood 2020;136:1330–41. https://doi.org/10.1182/blood.2020007252.
[47] Manne BK, Denorme F, Middleton EA, Portier I, Rowley JW, Stubben C, et al. Platelet gene expression and function in patients with COVID-19. Blood 2020;136:1317–29. https://doi.org/10.1182/blood.2020007214.
[48] Zhang S, Liu Y, Wang X, Yang L, Li H, Wang Y, et al. SARS-CoV-2 binds platelet ACE2 to enhance thrombosis in COVID-19. J Hematol Oncol 2020;13:120. https://doi.org/10.1186/s13045-020-00954-7.
[49] Le Joncour A, Biard L, Vautier M, Bugaut H, Mekinian A, Maalouf G, et al. Neutrophil–Platelet and monocyte–platelet aggregates in COVID-19 patients. Thromb Haemost 2020;120:1733–5. https://doi.org/10.1055/s-0040-1718732.
[50] D'Alessandro A, Thomas T, Dzieciatkowska M, Hill RC, Francis RO, Hudson KE, et al. Serum proteomics in COVID-19 patients: altered coagulation and complement status as a function of IL-6 level. J Proteome Res 2020;19:4417–27. https://doi.org/10.1021/acs.jproteome.0c00365.

[51] Arachchillage DRJ, Laffan M. Abnormal coagulation parameters are associated with poor prognosis in patients with novel coronavirus pneumonia. J Thromb Haemost 2020;18:1233–4. https://doi.org/10.1111/jth.14820.
[52] Sui J, Noubouossie DF, Gandotra S, Cao L. Elevated plasma fibrinogen is associated with excessive inflammation and disease severity in COVID-19 patients. Front Cell Infect Microbiol 2021;11:734005. https://doi.org/10.3389/fcimb.2021.734005.
[53] Fox SE, Akmatbekov A, Harbert JL, Li G, Quincy Brown J, Vander Heide RS. Pulmonary and cardiac pathology in African American patients with COVID-19: an autopsy series from New Orleans. Lancet Respir Med 2020;8:681–6. https://doi.org/10.1016/S2213-2600(20)30243-5.
[54] Jang H, Choudhury S, Yu Y, Sievers BL, Gelbart T, Singh H, et al. Persistent immune and clotting dysfunction detected in saliva and blood plasma after COVID-19. Heliyon 2023;9:e17958. https://doi.org/10.1016/j.heliyon.2023.e17958.
[55] Seth R, McKinnon TAJ, Zhang XF. Contribution of the von Willebrand factor/ADAMTS13 imbalance to COVID-19 coagulopathy. Am J Physiol Circ Physiol 2022;322:H87–93. https://doi.org/10.1152/ajpheart.00204.2021.
[56] Subramaniam S, Kothari H, Bosmann M. Tissue factor in COVID-19-associated coagulopathy. Thromb Res 2022;220:35–47. https://doi.org/10.1016/j.thromres.2022.09.025.
[57] Santiesteban-Lores LE, Amamura TA, da Silva TF, Midon LM, Carneiro MC, Isaac L, et al. A double edged-sword: the complement system during SARS-CoV-2 infection. Life Sci 2021;272:119245. https://doi.org/10.1016/j.lfs.2021.119245.
[58] Messner CB, Demichev V, Wendisch D, Michalick L, White M, Freiwald A, et al. Ultra-high-throughput clinical proteomics reveals classifiers of COVID-19 infection. Cell Syst 2020;11:11–24.e4. https://doi.org/10.1016/j.cels.2020.05.012.
[59] Perico L, Benigni A, Casiraghi F, Ng LFP, Renia L, Remuzzi G. Immunity, endothelial injury and complement-induced coagulopathy in COVID-19. Nat Rev Nephrol 2021;17:46–64. https://doi.org/10.1038/s41581-020-00357-4.
[60] Ramlall V, Thangaraj PM, Meydan C, Foox J, Butler D, Kim J, et al. Immune complement and coagulation dysfunction in adverse outcomes of SARS-CoV-2 infection. Nat Med 2020;26:1609–15. https://doi.org/10.1038/s41591-020-1021-2.
[61] Magro C, Mulvey JJ, Berlin D, Nuovo G, Salvatore S, Harp J, et al. Complement associated microvascular injury and thrombosis in the pathogenesis of severe COVID-19 infection: a report of five cases. Transl Res 2020;220:1–13. https://doi.org/10.1016/j.trsl.2020.04.007.
[62] Ma L, Sahu SK, Cano M, Kuppuswamy V, Bajwa J, McPhatter J, et al. Increased complement activation is a distinctive feature of severe SARS-CoV-2 infection. Sci Immunol 2021;6(59):eabh2259–2276. https://doi.org/10.1126/sciimmunol.abh2259.
[63] Brinkmann V, Reichard U, Goosmann C, Fauler B, Uhlemann Y, Weiss DS, et al. Neutrophil extracellular traps kill bacteria. Science 2004;303:1532–5. https://doi.org/10.1126/science.1092385.
[64] Szatmary P, Huang W, Criddle D, Tepikin A, Sutton R. Biology, role and therapeutic potential of circulating histones in acute inflammatory disorders. J Cell Mol Med 2018;22:4617–29. https://doi.org/10.1111/jcmm.13797.
[65] Li Y, Wan D, Luo X, Song T, Wang Y, Yu Q, et al. Circulating histones in sepsis: potential outcome predictors and therapeutic targets. Front Immunol 2021;12:650184. https://doi.org/10.3389/fimmu.2021.650184.
[66] Collier DM, Villalba N, Sackheim A, Bonev AD, Miller ZD, Moore JS, et al. Extracellular histones induce calcium signals in the endothelium of resistance-sized mesenteric arteries and cause loss of endothelium-dependent dilation. Am J Physiol Circ Physiol 2019;316:H1309–22. https://doi.org/10.1152/ajpheart.00655.2018.
[67] Westman J, Papareddy P, Dahlgren MW, Chakrakodi B, Norrby-Teglund A, Smeds E, et al. Extracellular histones induce chemokine production in whole blood ex vivo and leukocyte recruitment in vivo. PLoS Pathog 2015;11:e1005319. https://doi.org/10.1371/journal.ppat.1005319.
[68] Cascone A, Bruelle C, Lindholm D, Bernardi P, Eriksson O. Destabilization of the outer and inner mitochondrial membranes by core and linker histones. PLoS One 2012;7:e35357. https://doi.org/10.1371/journal.pone.0035357.
[69] Huckriede J, Anderberg SB, Morales A, de Vries F, Hultström M, Bergqvist A, et al. Evolution of NETosis markers and DAMPs have prognostic value in critically ill COVID-19 patients. Sci Rep 2021;11:15701. https://doi.org/10.1038/s41598-021-95209-x.
[70] Busch MH, Timmermans SAMEG, Nagy M, Visser M, Huckriede J, Aendekerk JP, et al. Neutrophils and contact activation of coagulation as potential drivers of COVID-19. Circulation 2020;142:1787–90. https://doi.org/10.1161/CIRCULATIONAHA.120.050656.
[71] Blasco A, Coronado M-J, Hernández-Terciado F, Martín P, Royuela A, Ramil E, et al. Assessment of neutrophil extracellular traps in coronary thrombus of a case series of patients with COVID-19 and myocardial infarction. JAMA Cardiol 2020;6:1–6. https://doi.org/10.1001/jamacardio.2020.7308.
[72] Shaw RJ, Abrams ST, Austin J, Taylor JM, Lane S, Dutt T, et al. Circulating histones play a central role in COVID-19-associated coagulopathy and mortality. Haematologica 2021;106:2493–8. https://doi.org/10.3324/haematol.2021.278492.
[73] Gould TJ, Lysov Z, Swystun LL, Dwivedi DJ, Zarychanski R, Fox-Robichaud AE, et al. Extracellular histones increase tissue factor activity and enhance thrombin generation by human blood monocytes. Shock 2016;46:655–62. https://doi.org/10.1097/SHK.0000000000000680.
[74] Ligi D, Lo Sasso B, Giglio RV, Maniscalco R, DellaFranca C, Agnello L, et al. Circulating histones contribute to monocyte and MDW alterations as common mediators in classical and COVID-19 sepsis. Crit Care 2022;26:260. https://doi.org/10.1186/s13054-022-04138-2.
[75] Middleton EA, He X-Y, Denorme F, Campbell RA, Ng D, Salvatore SP, et al. Neutrophil extracellular traps contribute to immunothrombosis in COVID-19 acute respiratory distress syndrome. Blood 2020;136:1169–79. https://doi.org/10.1182/blood.2020007008.
[76] Ng H, Havervall S, Rosell A, Aguilera K, Parv K, von Meijenfeldt FA, et al. Circulating markers of neutrophil extracellular traps are of prognostic value in patients with COVID-19. Arterioscler Thromb Vasc Biol 2021;41:988–94. https://doi.org/10.1161/ATVBAHA.120.315267.
[77] Cavalier E, Guiot J, Lechner K, Dutsch A, Eccleston M, Herzog M, et al. Circulating nucleosomes as potential markers to monitor COVID-19 disease progression. Front Mol Biosci 2021;8:600881. https://doi.org/10.3389/fmolb.2021.600881.
[78] Bouchard BA, Colovos C, Lawson MA, Osborn ZT, Sackheim AM, Mould KJ, et al. Increased histone-DNA complexes and endothelial-dependent thrombin generation in severe COVID-19. Vascul Pharmacol 2022;142:106950. https://doi.org/10.1016/j.vph.2021.106950.
[79] Sack GH. Serum amyloid A: a review. Mol Med 2018;24:46. https://doi.org/10.1186/s10020-018-0047-0.
[80] Li H, Xiang X, Ren H, Xu L, Zhao L, Chen X, et al. Serum amyloid A is a biomarker of severe coronavirus disease and poor prognosis. J Infect 2020;80:646–55. https://doi.org/10.1016/j.jinf.2020.03.035.
[81] Yu Y, Liu T, Shao L, Li X, He CK, Jamal M, et al. Novel biomarkers for the prediction of COVID-19 progression a retrospective, multi-center cohort study. Virulence 2020;11:1569–81. https://doi.org/10.1080/21505594.2020.1840108.
[82] Liu Y, Yan L-M, Wan L, Xiang T-X, Le A, Liu J-M, et al. Viral dynamics in mild and severe cases of COVID-19. Lancet Infect Dis 2020;20:656–7. https://doi.org/10.1016/S1473-3099(20)30232-2.
[83] He X, Lau EHY, Wu P, Deng X, Wang J, Hao X, et al. Temporal dynamics in viral shedding and transmissibility of COVID-19. Nat Med 2020;26:672–5. https://doi.org/10.1038/s41591-020-0869-5.
[84] Singh R, Rathore SS, Khan H, Karale S, Chawla Y, Iqbal K, et al. Association of obesity with COVID-19 severity and mortality: an updated systemic review, meta-analysis, and meta-regression. Front Endocrinol (Lausanne) 2022;13:780872. https://doi.org/10.3389/fendo.2022.780872.